FURTHER DEVELOPMENT OF THE BLOCKAGE TOLERANT WIND TUNNEL CONCEPT

M.J. Glanville and K.C.S. Kwok

The University of Sydney, School of Civil and Mining Engineering

Abstract

The University of Sydney boundary layer wind tunnel was converted into a tolerant type tunnel for testing 2D bluff bodies of high blockage. A surface singularity numerical investigation was used during the design of the tunnel. Pressure tapped bluff body models representing a 25% tunnel blockage were used to calibrate the completed tunnel. Correct pressure distribution over the models was achieved by using an optimal 'Open Area Ratio' and length of slatted ceiling. Pressure gradient measurements throughout the tolerant tunnel were made.

1. INTRODUCTION

Slatted wall tolerant wind tunnels are gaining in popularity since they provide an automatic and passive method for minimising the effects of blockage imposed by tunnel wall boundaries on large models. In a tolerant tunnel, the solid walls of the tunnel are replaced by longitudinally or transversely placed aerofoil section slats backed by a void plenum chamber.

The concept of the slatted wall tolerant tunnel arises from the fact that an open jet section and a closed jet section provide blockage correction of opposite sign. A slatted wall of evenly spaced aerofoil sections will act as an intermediate between the two jet configurations. A certain amount of flow is able to diverge into the plenum at the upstream end of a model and rejoin at the downstream end. Correct blockage tolerance is achieved when the resistance provided by the slatted wall matches the resistance that would be provided by an external unbounded flow.

Control of flow entering the plenum can be controlled by altering a number of degrees of freedom. Two of the most fundamental degrees of freedom are the Open Area Ratio (OAR) and the slatted wall length L_s. OAR is the percentage of slatted wall that is open to the plenum. This degree of freedom has been investigated by authors [2] [5] and [6]. An optimal OAR of 0.55 has been found to most effectively remove blockage errors for blockages up to 30%. Slatted wall length is another important degree of freedom affecting tolerant tunnel performance. This degree of freedom has received little attention to date and is investigated further in this paper.

In July 1995 the 2m high × 2.4m wide boundary layer wind tunnel (BLWT) at the University of Sydney was modified into a 2D tolerant type tunnel (Figure 1). A section of the tunnel ceiling was replaced by a transversely slatted wall so that large 2D models could be tested in boundary layer flow without pressure correction. This paper will describe the numerical design, construction and calibration of this tolerant tunnel.

2. PREVIOUS INVESTIGATIONS

Transversely slatted tolerant tunnels have been built and calibrated at the University of British Columbia in Canada [5], [7], [8] and [11], BRE in England [6] and Central Laboratories in New Zealand [2]. Performance of the BRE tunnel was not as good as expected. It was found that a small L_s/H ratio (slatted wall length / tunnel height) of 1.12 did not sufficiently reduce blockage effects. A numerical investigation of the Sydney University BLWT was thus made to determine an appropriate slatted ceiling length L_s.

3. NUMERICAL DESIGN

Surface singularity method [3] was used for the numerical design of the tolerant tunnel. Initially a numerical model was made of a half cylinder placed at the base of the tunnel amongst steady, irrotational flow. The distribution of C_p (coefficient of pressure) over the cylinder was calculated with and without a solid ceiling in place. The blockage ratio produced by the cylinder with the tunnel ceiling in place was modelled at 30%. The results presented in Figure 2 show perfect agreement with the ideal analytical case (solid line) for the free air configuration. An error of 20% can be seen at 30% blockage demonstrating the need for pressure correction with a solid ceiling in place.

An indirect method for calculating the required slatted ceiling wall length L_s is to alter a solid ceiling wall length L_w above the half cylinder numerical model and calculate the variation of C_p values at the apex of the cylinder. Figure 3 represents such a relationship for varying values of blockage ratio. The point at which the ceiling wall length L_w is seen to have no further affect upon the C_p value represents an appropriate slotted wall length L_s for a particular blockage ratio. An L_s/H value of 4 is seen to be suitable at 30% blockage. This is equivalent to an 8m slatted ceiling wall length in the Sydney University BLWT.

4. MODIFICATION OF THE EXISTING BLWT

A 9m long transversely slatted ceiling backed by a plenum chamber was installed above the BLWT. Figure 1 illustrates the final configuration of the tolerant tunnel in its exiting state. Slatted ceiling length L_s can be adjusted by placing pegboard panels (porosity 5%) at either end of the plenum, and symmetrically about the centre of the plenum, as shown in Figure 1. Plenum depth is restricted to about 0.47m by the roof of the laboratory.

NACA0015 aerofoil sections machined from ramin timber constitute the slatted ceiling. Each foil is of 89mm chord length inclined at zero angle of incidence. The foils span the width of the tunnel at 2.4m. Spacing between each foil can be altered to adjust the OAR.

5. TUNNEL CALIBRATION

5.1 Experimental Arrangement

Mean pressure distribution over a 2D half cylinder and step model was used to calibrate the tunnel. Both models were built from smooth timber veneer and represented a 25% blockage in the tunnel. The half cylinder model had a cross-sectional radius of 0.5m while the step model had a rectangular cross sectional area of 0.5m × 1.17m. Both models spanned the width of the tunnel at 2.4m. The models were placed on the floor of the tunnel beneath the centre of the slatted ceiling. Figure 4 shows the wind velocity and turbulence intensity profiles at the model locations. These profiles were generated by a fetch of polished masonite boards.

An array of pressure tappings were evenly spaced over the central portions of each model. Pressure taps were connected to a Scanivalve switching mechanism which linked each tap to a Honeywell low pressure transducer. Mean pressure coefficient $C_{p\,mean}$ was calculated as follows:

$$C_{p\,mean} = \frac{\overline{p}_{tap} - \overline{p}_{static}}{\frac{1}{2}\rho\, U_o^2}$$

where

$\overline{p}_{tap}$ = Mean tap pressure

$\overline{p}_{static}$ = Mean reference static pressure

ρ = Air density at atmospheric pressure

U_o = Mean reference flow velocity

Reference pressures were measured using a pitot tube placed 4.5m upstream of the model centre at a height of 0.5m. The pitot tube was connected to a Honeywell low pressure transducer. The same pitot tube was used to measure static and dynamic pressure gradients along the mid height centre line of the tunnel (Figure 1) and inside the plenum chamber.

5.2 Experimental Results

Measured mean pressure coefficients $C_{p\ mean}$ over the half cylinder model are plotted in Figure 5 for varying L_s/H ratios. During this test the OAR and Reynolds number were maintained at 0.55 and 1×10^6 respectively. Included in the figure are blockage free $C_{p\ mean}$ values for half cylinder models in boundary layer flow as obtained from the investigations of Ogawa et al [4] and Toy and Tahouri [10]. Both of these investigations were performed at Reynolds numbers less than 1×10^6. It is considered that comparison with these results is still permissible since mean pressure coefficients over the half cylinder model in boundary layer flow were found to be Reynolds number independent.

An L_s/H ratio of about 2.5 provides the best agreement with the blockage free measurements of [4] and [10]. At L_s/H ratios less than 2.5, the short slatted ceiling length is unable to provide adequate divergence of flow into the plenum. Flow is constrained between the tunnel ceiling and the model thereby inducing excessively high negative pressures ($C_{p\ mean}$ values) over the cylinder. Alternatively, as the L_s/H ratio is opened beyond 2.5, the tunnel assumes open jet behaviour. Flow prematurely enters the plenum well upstream and independently of the model. Excessive flow into the plenum reduces flow in the tunnel and around the model. Thus there is a difference between the reference velocity U_o upstream of the plenum and velocity in the vicinity of the model. The result is an *apparent* overcompensation in $C_{p\ mean}$ values at high L_s/H.

Figure 6 plots the piezometric head in dimensionless form along the centre line of the tunnel with the half cylinder model in place. The relative variation in static and dynamic pressure intensity along the tunnel is shown for various L_s/H ratios. A distinct increase in static pressure corresponding to a decrease in dynamic pressure (or velocity) is seen well upstream of the model at high L_s/H ratios. This occurs as flow prematurely expands into the plenum. When the plenum is completely closed ($L_s/H = 0$), the static pressure over the model is too low (velocity too high). The optimal slatted ceiling length ($L_s/H = 2.5$) prevents flow from prematurely entering the plenum yet does not restrict the flow over the model. Piezometric head along the centre line of the tunnel is also shown for zero tunnel blockage and $L_s/H = 2.5$ in Figure 6. There is a desirably small pressure gradient at the optimal slatted ceiling length when the tunnel is empty.

Unfortunately there is a notable drop in piezometric head over the half cylinder model at the optimal L_s/H ratio as shown in Figure 6. This can be ascribed to upstream back pressure induced by the model's 25% blockage. This caused $C_{p\ mean}$ values on the leeward side of the half cylinder model to be more negative than the blockage free calibration values of [4] and [10] as shown in Figure 5.

It was anticipated that reducing the foil spacings (reducing the OAR) might reduce excess flow entering the plenum at high L_s/H ratios. Pressure gradient measurements were then performed for the configuration $L_s/H = 4.5$ and OAR = 0.4 with the half cylinder model in place. The results shown in Figure 7 indicate that excessive flow divergence into the plenum is only slightly reduced by using the lower OAR. Reducing the OAR below 0.4 will restrict model induced flow into the plenum [5].

Flow inside the plenum chamber was also measured for varying L_s/H and OAR. Dynamic pressure inside the plenum along a level 150mm above the slatted ceiling is shown in Figure 8 with the half cylinder model in place. Maximum flow is induced into the plenum at high L_s/H and OAR values as expected. Dynamic pressure along the same plenum level is also shown in Figure 8 with the half cylinder model removed from the tunnel. Flow does not enter the plenum at zero tunnel blockage for the optimum tunnel configuration ($L_s/H = 2.5$ and OAR = 0.55).

Mean pressure coefficients measured over the 0.5 x 1.17 m rectangular step model are shown in Figure 9. At the optimum tunnel configuration negative $C_{p\ mean}$ pressure coefficients were found to be greater than those values obtained by Surry [9] at low blockage. Increasing the OAR to 1 by removing the foils decreased the minimum $C_{p\ mean}$ value from -1.65 to -1.4 at $L_s/H = 2.5$. This value however was still

greater than Surry's reference coefficient. A similar problem was encountered by Broughton et al [1] when testing sharp edged block models in a longitudinally slatted tolerant tunnel. They found that long and sharp edged body shapes (having a closed separation bubble) do not perform well in tolerant tunnels.

6. CONCLUSIONS

The University of Sydney boundary layer wind tunnel was modified into a tolerant type tunnel for testing 2D bluff bodies of high blockage. A surface singularity numerical investigation was used to aid in the design of the modifications.

A 9m slatted ceiling backed by a plenum chamber was installed as a result of the numerical investigation. This represented a slatted ceiling length to tunnel height ratio (L_s/H) of 4.5 which was found to be too long. In real tunnel flow, an optimal L_s/H ratio of 2.5 was found for an Open Area Ratio (OAR) of 0.55. The optimal plenum length prevents flow from prematurely entering the plenum yet does not restrict flow over a model of significant blockage. Flow does not enter the plenum when there is zero blockage in the tunnel at the optimum plenum length. Reducing the Open Area Ratio below 0.55 did not prevent the tunnel from behaving as an open jet at high L_s/H ratios and high blockage.

At the optimum tolerant tunnel configuration ($L_s/H = 2.5$ and OAR = 0.55), mean pressure coefficients over the windward and top face of a half cylinder model (25% blockage) were the same as blockage-free reference coefficients. Pressure coefficients on the leeward side of the model were too high due to a static pressure gradient.

The tolerant tunnel significantly reduced blockage induced errors in mean pressure coefficients over a step model of 25% blockage.

ACKNOWLEDGMENTS

The authors wish to acknowledge S.M.J Premnath for his involvement with the numerical investigation. Particular thanks go to Paul Donovan who performed much of the tunnel modifications including the alteration of a 250 Kg portal frame beam that was originally protruding through the plenum. Mark Maclean and Roy Denoon were also involved with the tunnel modifications.

REFERENCES

1. Broughton,C.A., Rainbird,W.J., and Kind,R.J., "An experimental investigation of interference effects of high blockage bluff bodies in a slotted-wall wind tunnel section", Journal of Wind Engineering and Industrial Aerodynamics", Vol 56, pp23-39, 1995.
2. Carpenter, P., "Development of a blockage-tolerant wind tunnel to minimise blockage effects", Central Laboratories Report 92-29129, 1992.
3. Hess, J.L., and Smith, A.M.O., "Calculation of potential flow about arbitrary bodies", Progress in Aeronautical Sciences, Vol 8, Pergamon Press, 1966.
4. Ogawa, T., Nakayama, M., Murayama, S., and Sasaki, Y., "Characteristics of wind pressures on basic structures with curved surfaces and their response in turbulent flow", Journal of Wind Engineering and Industrial Aerodynamics, Vol 38, pp.427-438, 1991.
5. Parkinson, G.V., "Tolerant tunnel-concept and performance", Canadian Aeronautics and Space Journal, Vol 36 No.3, pp.130-134, 1990.
6. Parkinson, G.V., and Cook, N.J., "Blockage tolerance of a boundary layer wind tunnel", Journal of Wind Engineering and Industrial Aerodynamics, Vol 41-44, pp.873-884, 1992.
7. Parkinson, G.V., and Hameury, M., "Performance of the tolerant wind tunnel for bluff body testing", Japanese Journal of Wind Engineering, Vol 37, 1988.
8. Premnath, S.M.J., and Parkinson, G.V., "A tolerant tunnel for axi-symmetric testing", Proc.IV Asian Congress of Fluid Mechanics, Hong Kong, 1989.
9. Surry, D., "Pressure measurements on the Texas Tech building: wind tunnel measurements and comparisons with full scale", Journal of Wind Engineering and Industrial Aerodynamics, Vol 38, pp.235-247, 1991.
10. Toy, N. and Tahouri, B., "Pressure distributions on semi-cylindrical structures of different geometrical cross-sections", Journal of Wind Engineering and Industrial Aerodynamics, Vol 29, pp.263-272, 1988.
11. Williams, C.D., Parkinson, G.V., and Malek, A., "Development of a low correction wind tunnel wall configuration for testing high-lift aerofoils.", Proceedings of the eleventh Congress I.C.A.S, Lisbon, 1978.

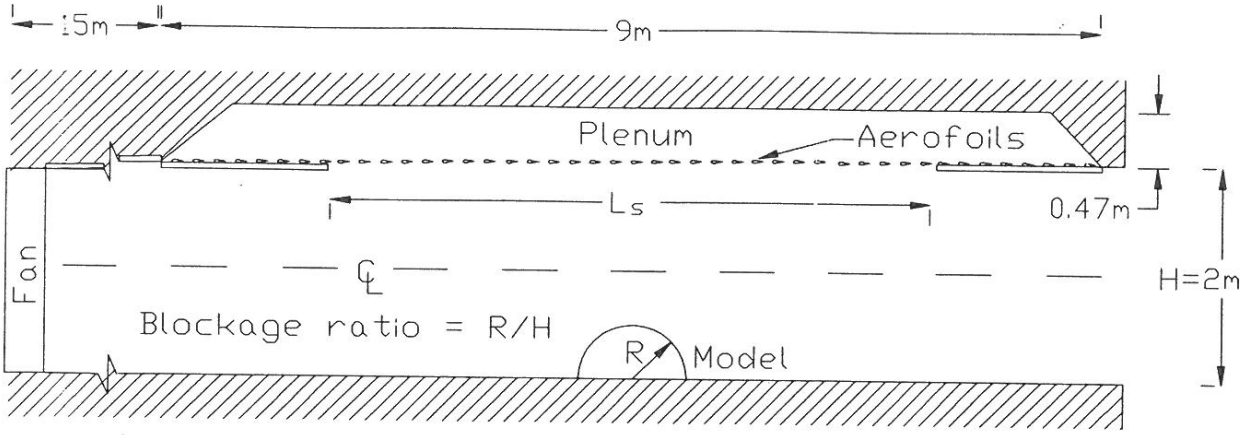

Figure 1: Elevation of the Sydney University tolerant tunnel.

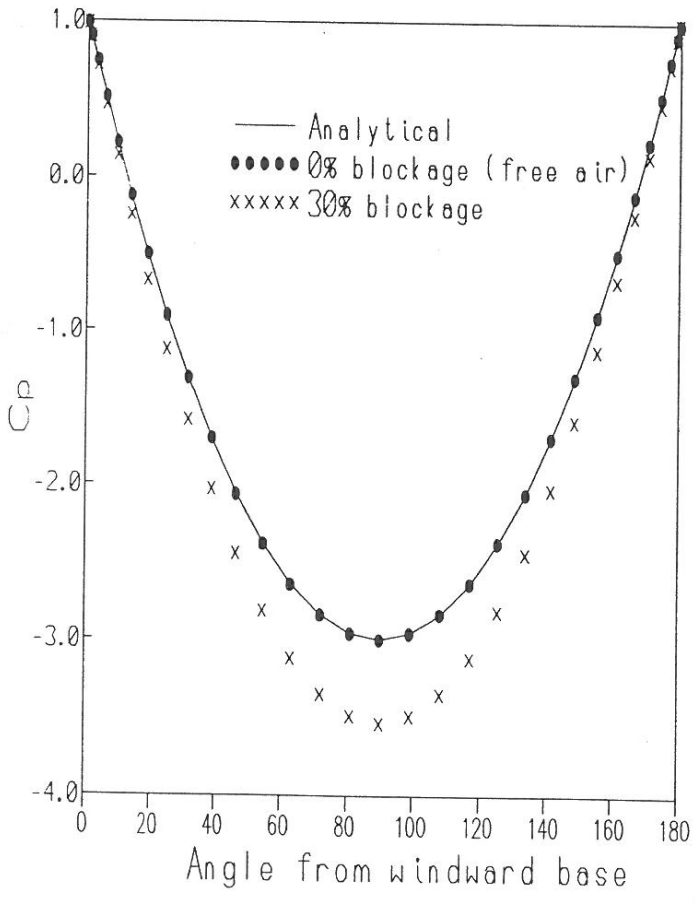

Figure 2: Pressure distribution over a half cylinder in ideal flow

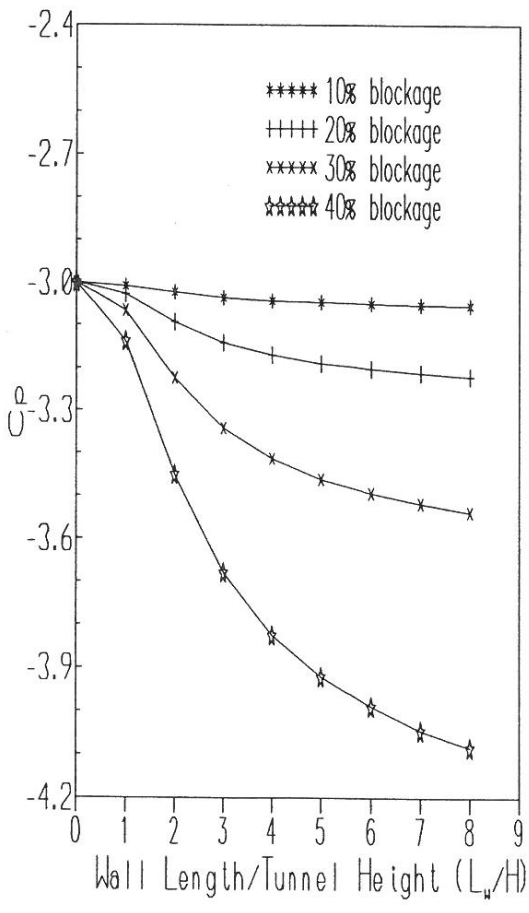

Figure 3: Variation of the numerical C_p value with tunnel ceiling wall length L_w

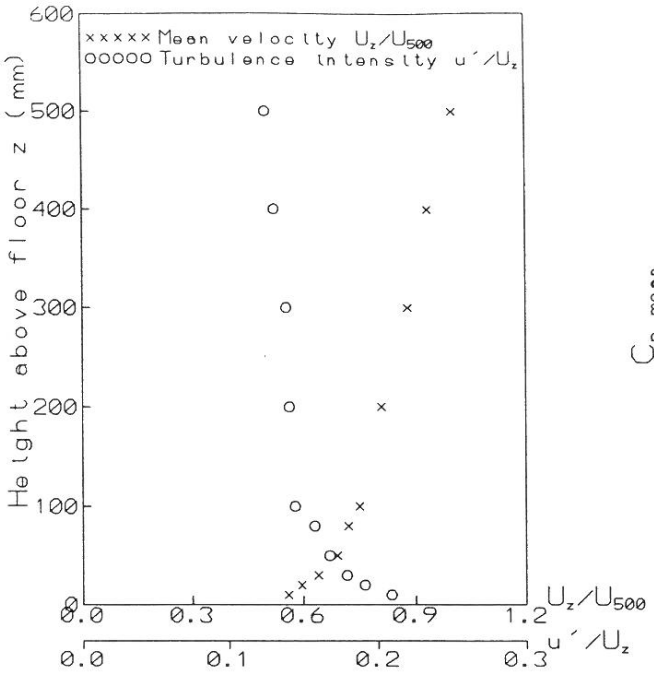

Figure 4: Approach-flow mean velocity and turbulence intensity profiles

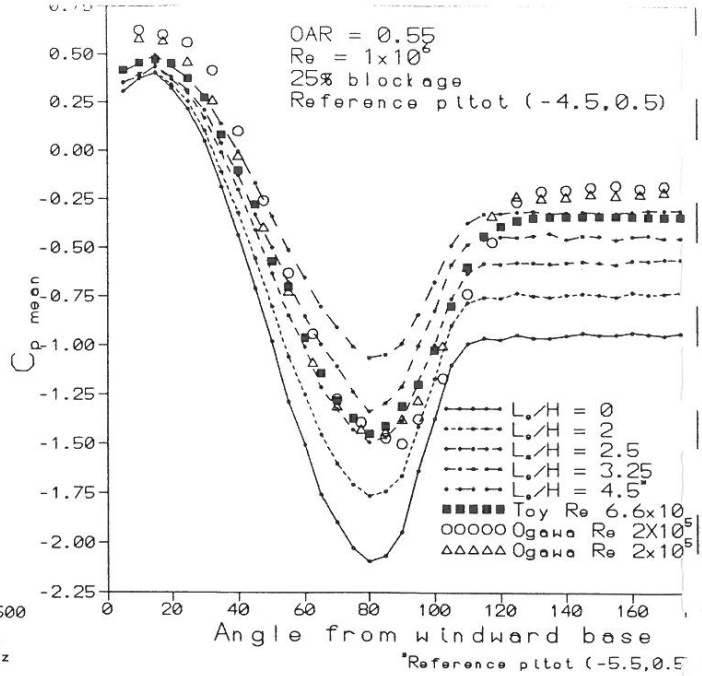

Figure 5: Mean pressure coefficient distribution over a half cylinder model for varying L_s/H

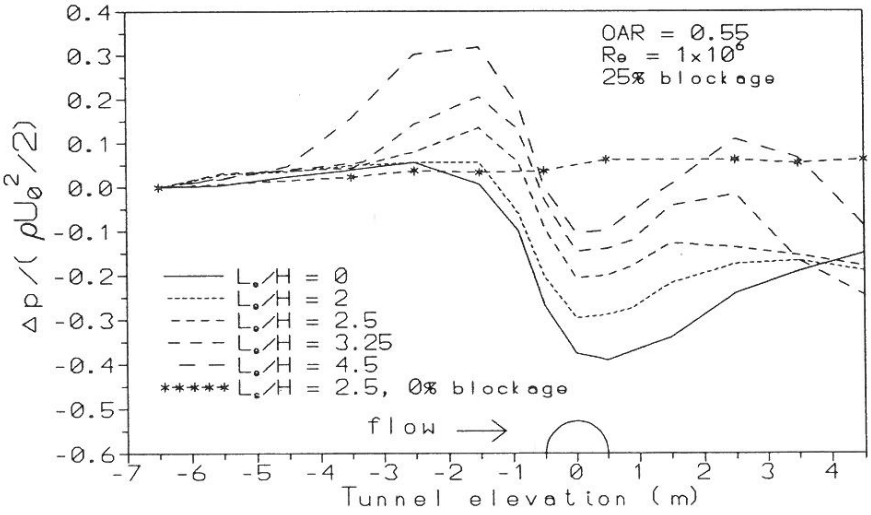

Figure 6: Variation of piezometric head along the tolerant tunnel centre line for varying L_s/H

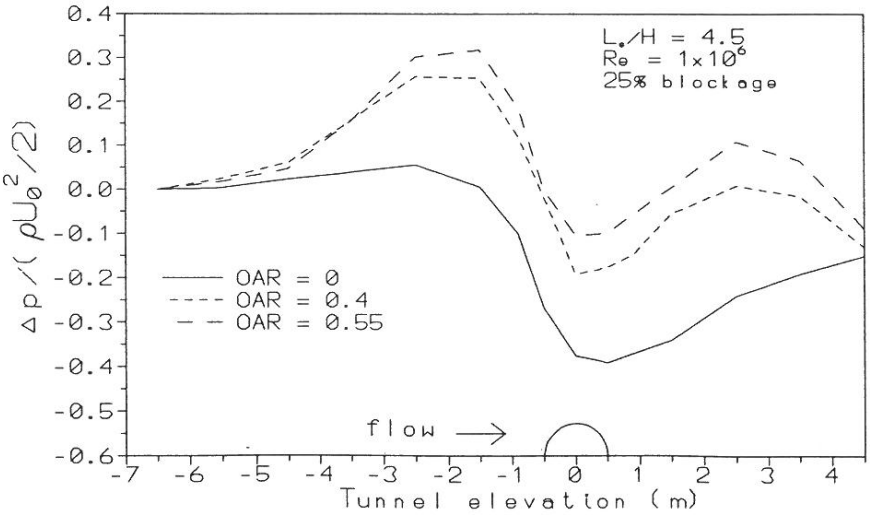

Figure 7: Variation of piezometric head along the tolerant tunnel centre line for varying OAR

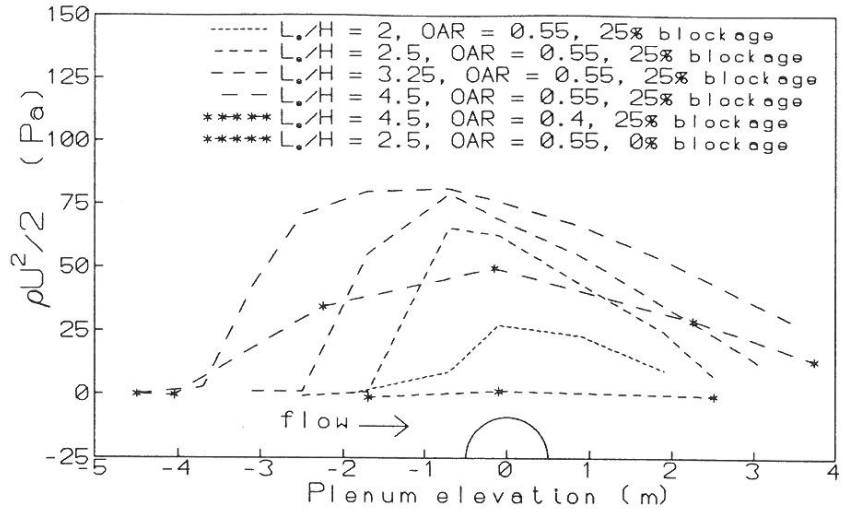

Figure 8: Dynamic pressure in plenum, 150mm above slatted ceiling

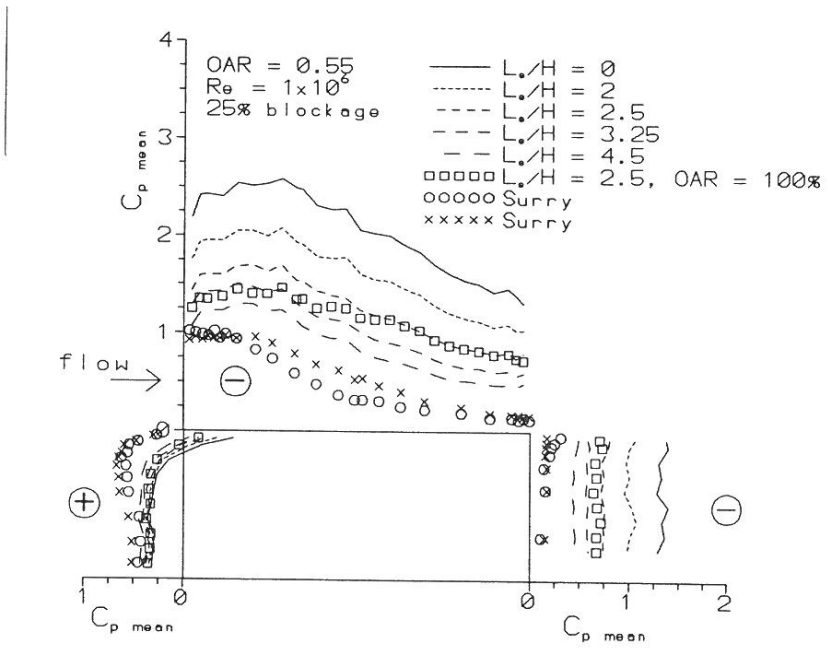

Figure 9: Mean pressure coefficient distribution over a step model for varying L_s/H